Strange nonchaotic attractors in the quasiperiodically forced logistic map

Awadhesh Prasad, Vishal Mehra, and Ramakrishna Ramaswamy
School of Physical Sciences, Jawaharlal Nehru University, New Delhi 110 067, India
(Received 4 September 1997)

Different mechanisms for the creation of strange nonchaotic dynamics in the quasiperiodically forced logistic map are studied. These routes to strange nonchaos are characterized through the behavior of the largest nontrivial Lyapunov exponent, as well as through the characteristic distributions of finite-time Lyapunov exponents. Strange nonchaotic attractors can be created at a saddle-node bifurcation when the dynamics shows type-I intermittency; this *intermittent* transition, which is studied in detail, is characterized through scaling exponents. Band-merging crises through which dynamics remains nonchaotic are also studied, and correspondence is made with analogous behavior in the unforced logistic map. Robustness of these phenomena with respect to additive noise is investigated. [S1063-651X(98)10302-1]

PACS number(s): 05.45.+b

I. INTRODUCTION

Of the diverse structures that are found in nonlinear dynamical systems, strange nonchaotic attractors (SNAs) are among the more exotic. These were described by Grebogi *et al.* [1] in the context of quasiperiodically forced systems, and are characterized by having a geometrically strange structure (usually a fractal, which is everywhere single valued but piecewise nondifferentiable) with ''nonchaotic'' dynamics: the largest nontrivial Lyapunov exponent Λ is negative, and nearby orbits do not diverge from each other exponentially. Since they were described [1], a number of characteristics of SNAs have been studied theoretically [2–13] and experimentally [14–16].

Strange nonchaotic dynamics usually occurs in the vicinity of strange chaotic behavior and periodic or quasiperiodic (nonstrange, nonchaotic) behavior. The different mechanisms through which SNAs are created, either from regular or from chaotic motion, and the mechanisms through which they disappear, either into regular or chaotic motion—the birth and death of strange nonchaotic attractors, so to speak—is a topic of considerable current interest.

In this paper we address this question in the context of a typical dynamical system with quasiperiodic forcing and discuss a number of transitions in such systems. These include, apart from the transition from quasiperiodic or chaotic motion to strange nonchaotic dynamics, transitions between different SNAs.

We study the quasiperiodically forced logistic map which is given by the equations

$$x_{n+1}=\alpha[1+\epsilon\cos(2\pi\phi_n)]x_n(1-x_n),$$

$$\phi_{n+1}=\phi_n+\omega \pmod 1,$$

where $x\in R^1$, $\phi\in S^1$, $\omega=(\sqrt{5}-1)/2$ is the irrational driving frequency, and ϵ represents the forcing amplitude. With quasiperiodic driving the periodic attractors of the logistic map become quasiperiodic attractors, and following the standard notation [5], we denote a torus attractor of period n in $R^1\times S^1$ as n-T.

Four mechanisms or scenarios for the creation of SNAs in quasiperiodically driven systems have been advanced. In the absence of quasiperiodic forcing, the corresponding systems show the by now standard scenarios for the route to chaotic or aperiodic behavior, including quasiperiodicity, period-doubling and tangent bifurcations, intermittency, crises, and band-merging or reverse bifurcations [17]. There are parallels to several of these in the different routes to SNAs.

(1) Heagy and Hammel [5] identified the birth of a SNA with the collision between a period-doubled torus and its unstable parent. This mechanism requires that a period-doubling bifurcation occur, after which the stable torus attractor gets progressively more ''wrinkled'' as the parameters in the system change, i.e., $x(\phi)$ becomes more and more oscillatory. Following a collision with the unstable parent torus, at an analog of the attractor-merging crisis that occurs in chaotic systems [2], the SNA is born. Λ remains negative throughout the collision process. This mechanism, which we denote by HH in the remainder of this paper, has been seen both for a period-2 torus as well as for the period-4 torus; the quasiperiodic forcing drives the system into chaos well before the infinite sequences of period doubling can occur.

(2) The ''fractalization'' route for the creation of SNAs has been described by Nishikawa and Kaneko [6,7]. A torus gets increasingly wrinkled and transforms into a SNA without any interaction with a nearby unstable periodic orbit. This route to SNA (and eventually to chaos) has also been observed in higher-dimensional systems [11].

(3) In the intermittency scenario for the formation of SNAs [18], as a function of driving parameter a strange attractor disappears and is eventually replaced by a one-frequency torus through an analog of the saddle-node bifurcation. In the vicinity of this crisislike phenomenon [2] the attractor is strange and nonchaotic. We have shown that the dynamics at this transition shows scaling behavior characteristic of type-I intermittency [13], and the signature of the transition is an abrupt and characteristic change in the variation of Λ. The intermittent route is a general one which can be found in other systems as well [19].

(4) Yalçinkaya and Lai [8] identify the birth of SNAs with a blowout bifurcation [9], when a torus loses transverse stability. The Lyapunov exponent also has a characteristic dependence on parameter in this case.

SNAs can be quantitatively characterized by a variety of methods, including the estimation of the Lyapunov exponents and the fractal dimension [1,3,20], spectral properties [3,7], and examination of the time series [11,21]. The geometric strangeness of the attractor can be measured through indices such as the phase-sensitivity exponent [10], while the chaoticity properties can be studied by examining the finite-time Lyapunov exponents [10,18].

A number of transitions in this system are investigated wherein three of the above mechanisms for the creation of SNAs are known to be operative (blowout bifurcations cannot occur), notably the processes whereby SNAs are created from torus (T) attractors,

$$\cdots nT \leftrightarrow n \text{ band SNAs} \leftrightarrow \cdots, \tag{2}$$

$$2^n T \leftrightarrow 2^{n-1} \text{ band SNAs} \leftrightarrow \cdots, \tag{3}$$

or others, such as from SNA to chaotic attractors (C) or from a k-band SNA to a $k/2$-band SNA,

$$\cdots n \text{ band SNAs} \leftrightarrow n \text{ band } C \leftrightarrow \cdots, \tag{4}$$

$$\cdots \leftrightarrow k \text{ band SNAs} \leftrightarrow k/2 \text{ band SNAs} \leftrightarrow k/2 \text{ band } C \leftrightarrow \cdots. \tag{5}$$

The latter class of bifurcations (for k a power of 2) is studied here through analysis of the Lyapunov exponents and their distributions. We also explore the effect of additive noise.

This paper is organized as follows. In Sec. II, we describe the ''phase diagram'' for the forced logistic map: the regions corresponding to the different dynamical behavior that obtain are delineated as a function of parameters. This phase diagram is canonical for dynamical systems such as Eq. (1), namely, unimodal maps that are parametrically driven, and generalizes the usual bifurcation diagram that is obtained in the absence of forcing. Transitions to SNAs and the characteristic behavior of the Lyapunov exponents are discussed in Sec. III, where we also discuss other transformations that are undergone by SNAs, such as the analog of band merging. The creation of SNAs is often accompanied by intermittent dynamics, and this can be quantitatively described in terms of scaling exponents at these transitions. These results are also given in Sec. III, where we discuss, in addition, the effects of additive noise. This is followed by a summary in Sec. IV.

II. FORCED LOGISTIC MAP: PHASE DIAGRAM

The quasiperiodically forced logistic map [5] is particularly convenient for study since the phenomenology is smoothly related to that of the logistic map in the limit of $\epsilon \to 0$. Since x and ϕ are uncoupled in this limit, the period-k orbits of the logistic map are converted into k-frequency tori, and the chaotic attractors in the logistic map appear as chaotic band attractors of the two-dimensional map, Eq. (1).

The region of interest in the phase space is $0 \leqslant x \leqslant 1$, $0 \leqslant \phi \leqslant 1$. For $\epsilon \neq 0$, it is clear that motion will remain bounded in this region so long as $\alpha[1+\epsilon\cos(2\pi\phi_n)] \in [0,4]$. Thus for any $\alpha \leqslant 4$, the largest value of ϵ allowed is $4/\alpha - 1$. We therefore redefine the driving parameter as $\epsilon' = \epsilon/(4/\alpha - 1)$ and study the system for $0 \leqslant \epsilon' \leqslant 1$.

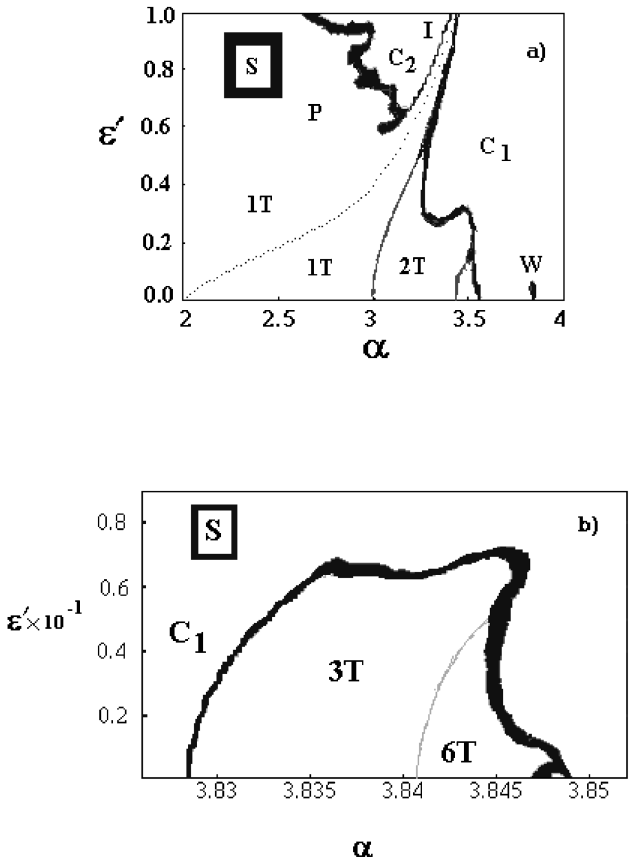

FIG. 1. (a) Phase diagram for the forced logistic map (schematic). The rescaled parameter ϵ' is defined as $\epsilon' = \epsilon/(4/\alpha - 1)$. T and C correspond to torus and chaotic attractors. The shaded region along the boundary of T and C corresponds to SNA (marked S). The boundaries separating the different regions are convoluted, and regions of SNA and chaotic attractors are interwoven in a complicated manner. The dashed curve marks the locus of the ''superstable'' orbit (see the text). The region of periodic attractors can be further demarcated into period-1, -2, and -4 tori as shown ($1T$, $2T$, and $4T$). W denotes the window of periodic behavior corresponding to the period-3 orbit of the logistic map. This is shown enlarged in Fig. 1(b). Intermittent SNAs are found on the edge of the C_2 region marked I, while the left boundary of C_2 has only fractalized SNAs. Along the boundary of C_1, both fractalized and HH SNAs can be found. (b) An enlargement of the window W indicated in (a). This small window shows periodic tori of period 3,6, . . . and their SNAs that are created either through the Heagy-Hammel process or fractalization. As may be expected, other similar windows can be seen upon further enlargement.

Figure 1 is a phase diagram [18] of the system as a function of α and ϵ'. (The regime $\alpha \leqslant 2$ is featureless and uninteresting.) The different possible dynamical behavior—periodic, strange nonchaotic, and chaotic attractors, corresponding to the symbols P, S and C in the phase diagram—are characterized through the largest nonzero Lyapunov exponent,

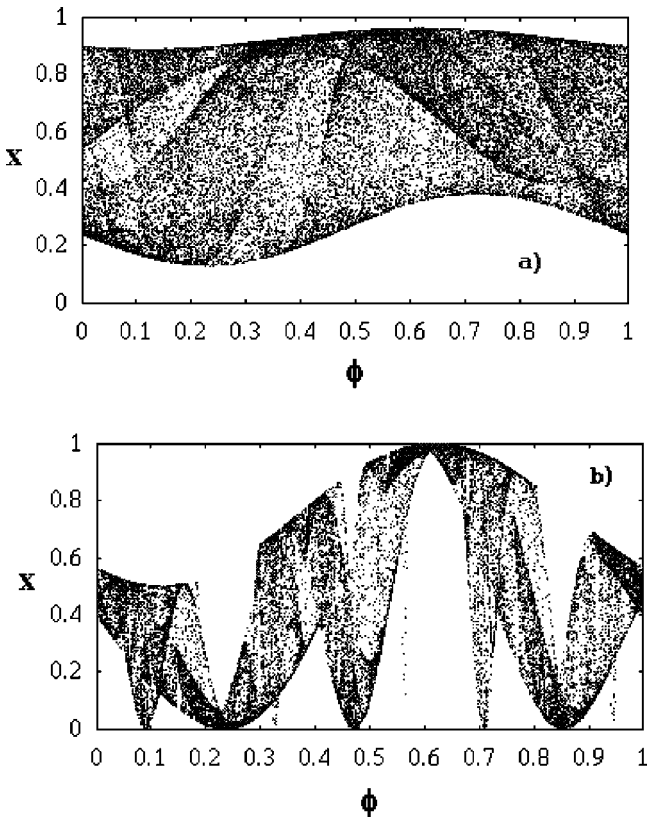

FIG. 2. Typical chaotic attractors in the two regions (a) C_1, for $\alpha=3.6$, $\epsilon'=0.5$, and (b) C_2 at $\alpha=3$, $\epsilon'=1$.

$$\Lambda=\lim_{N\to\infty}\frac{1}{N}\sum_{i=1}^{N}\ln|\alpha[1+\epsilon\cos(2\pi\phi_i)](1-2x_i)|. \quad (6)$$

We calculate Λ typically from 10^6 iterations of the map (after removing transients for 10^5 iterations) which is sufficient to converge the results to within 10^{-4}. To obtain Fig. 1, Λ has been calculated in a 100×100 grid, and the boundaries of the chaotic regions are determined from the $\Lambda=0$ contour.

The main interesting feature of this phase diagram is the presence of two separate chaotic regimes, C_1 and C_2. The C_1 region is the continuation of the chaotic regime in the logistic map (this appears, for $\epsilon=0$ at the end of the period-doubling cascade, at $\alpha=3.5699\ldots$). The superstable orbit which exists at $\epsilon=0,\alpha=2$ continues (slightly distorted) for nonzero ϵ' along the locus $\epsilon'\approx2(1-2/\alpha)/5(4/\alpha-1)$; this line [the dotted curve in Fig. 1(a)] separates C_1 and C_2. The latter chaotic region is one of low nonlinearity and large-amplitude forcing. The two types of chaotic attractors that occur in these two regions are qualitatively quite different—see Figs. 2(a) and 2(b).

SNAs are found in the vicinity of the boundaries of the chaotic regions, where $\Lambda<0$. The different mechanisms through which they are formed in different regions are discussed below.

Along the left edge of the region C_2, for $0.59\leqslant\epsilon'\leqslant1$, the route to SNA is through fractalization. This region lies to the left of the curve of ''superstable one-torus'' points [the dashed line in Fig. 1(a)], namely, well before torus doubling occurs. For fixed ϵ', SNAs are created through fractalization in an interval in α as indicated in the phase diagram.

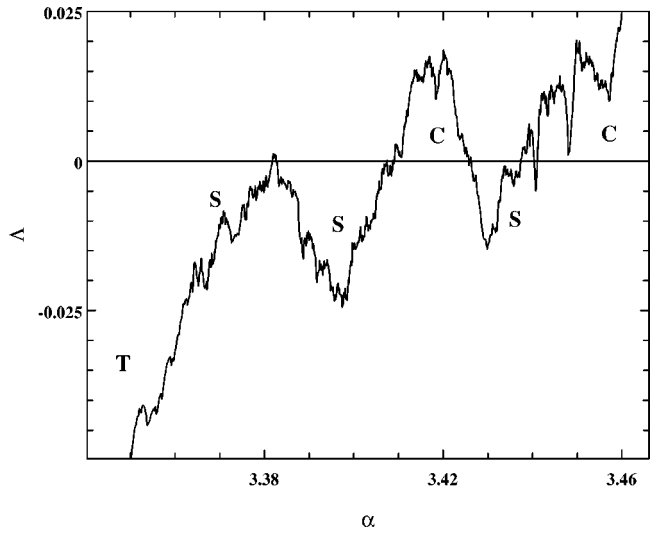

FIG. 3. Variation of Λ as a function of α for fixed $\epsilon=0.05$. Note the highly oscillatory structure indicative of several transitions in the system.

Along the right edge of C_2, SNAs are born through *intermittency*. Consider a superstable one-torus. In the regime $0.59\leqslant\epsilon'\leqslant1$, as α is decreased, holding ϵ' fixed, a saddle-node bifurcation takes place and the torus becomes a SNA, eventually becoming a chaotic attractor. This process occurs over a somewhat narrow range of parameters as compared to the other routes discussed in Sec. I.

Along the left edge of C_1 SNAs are created either via the HH mechanism, or through fractalization. The phenomenon of truncation or interruption of the period-doubling cascade resulting from the quasiperiodic driving was noted by Kaneko [22], who also showed that there was a power-law scaling between the number of doublings and the driving amplitude. The requirement, in the Heagy-Hammel mechanism, that a period-doubled torus collide with its unstable parent, is a stringent one, and this is achieved only for selected parameter intervals. Fractalization is also a likely cause for the interruption of period doubling [22]. The actual mechanism through which a SNA is created is easily identified from the morphology of the attractor: a k-torus gives rise to a $k/2$-band SNA in the Heagy-Hammel mechanism, and to a k-band SNA through fractalization. At low forcing amplitude the fractalization is found to be dominant while the HH mechanism is more common at higher forcing. In particular, we do not find any fractalization event above $\epsilon'\sim0.7$.

The regions of SNA are quite complicated. The boundaries between chaotic attractors and SNAs are convoluted, with regions of torus attractors interspersed among the regions of SNAs. Thus there are several transformations that the attractors of this system undergo apart from the birth and death mechanisms, namely, the transition from torus to SNA or SNA to chaos. Indeed, along a line of constant ϵ or constant ϵ', Λ is highly nonmonotonic and reveals a number of bifurcations. An example is shown in Fig. 3, for constant $\epsilon=0.05$. Clearly, there are transitions from $T\to$SNA$\to$chaos $\to$SNA$\to$chaos . . . , finally terminating in the C_1 chaotic region.

Within the SNA region, there are transitions from 2^n-band SNAs to 2^{n-1}-band SNAs. At these transitions again there are distinctive and unusual signatures in the dependence of Λ, as well as in the distribution of finite-time Lyapunov exponents. This is discussed in the following section.

Compared to the system at $\epsilon=0$, for nonzero ϵ it is usually possible to observe regular motion only on n-T with $n=1,2,3,4,6,8,16$. Higher n-frequency tori are surely present, but the regions where they occur are extremely narrow. The period-3 window of the logistic map extends as a narrow region of stability wherein one can locate 3-T, 6-T, and the associated SNAs, which are formed through the same general mechanisms as outlined in Sec. I. An enlargement of this region of the phase diagram [marked by W in Fig. 1(a)] is shown in Fig. 1(b). The three-band and six-band SNAs that occur appear to be formed through the fractalization or Heagy-Hammel route.

This qualitative picture appears to be valid for all quasiperiodically forced unimodal maps. We have studied the additively forced logistic map, as well as the forced sine map, and found a similar phase diagram. For higher-dimensional systems, the picture gets somewhat more complicated, but the essential qualitative features carry over, much in the same manner as the bifurcation diagram for one-dimensional (1D) maps generalizes for higher-dimensional dissipative chaotic systems. This system is also not very sensitive to the numerical value of the irrational driving frequency ω: qualitatively similar phase diagrams have been obtained for other ω's.

III. RESULTS AND DISCUSSION

In this section we study the variation of the dynamics through several transitions in the system as the parameters α and ϵ are varied. In addition to the Lyapunov exponent Λ itself, we also examine the N-step Lyapunov exponents, λ_N, namely,

$$\lambda_N=\frac{1}{N}\sum_{i=1}^{N}\ln|\alpha[1+\epsilon\cos(2\pi\phi_i)](1-2x_i)|, \tag{7}$$

their variance σ, and the distribution

$$P(N,\lambda)d\lambda=(\text{probability that } \lambda_N \text{ lies between } \lambda \text{ and } \lambda+d\lambda). \tag{8}$$

This is of great relevance when studying the stability of systems where a small change in control parameter gives rise to drastic change in dynamical behavior. In our calculations, Λ and its variance are typically computed from a sample of 50 estimations of step length $N=10^5$.

The SNA→chaos route, which has been studied extensively and where it is known that the Lyapunov exponent varies linearly through the transition [12], will not be considered here.

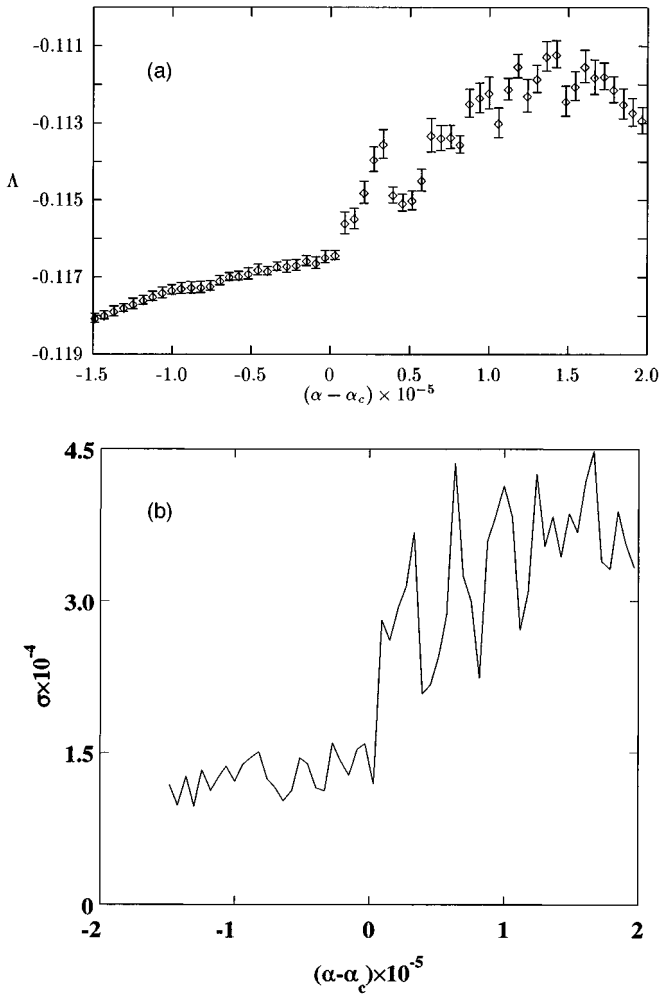

FIG. 4. The transition from a period-2 torus to one-band SNA through the Heagy-Hammel mechanism along the line $\epsilon'=0.3$ and at $\alpha_{\rm HH}=3.487\,793\ldots$. (a) Behavior of Λ through the transition, and (b) the variance.

A. From tori to SNAs

1. The Heagy-Hammel mechanism

In the HH mechanism [5], a period-2^n torus attractor gets wrinkled and upon collision with the parent unstable period-2^{n-1} torus, a 2^{n-1}-band SNA is formed. This phenomenon is similar (in some sense) to the band-merging crisis that occurs in unforced systems, where the Lyapunov exponent is known to have a discontinuous slope [23]. In contrast, in Ref. [5] the transition to SNA appeared to be smooth as a function of the parameter (see Figs. 2 and 10 in [5]).

We examine this behavior in some detail in Fig. 4(a), where for $\epsilon'=0.3$ the crisis takes place at $\alpha_{\rm HH}=3.487\,793\ldots$. When examined in a sufficiently small neighborhood of α_c, the transition is clearly revealed by Λ: on the torus, Λ varies smoothly but in the SNA phase the variation is rather irregular and the crossover between these two behaviors is abrupt. It is also possible to identify the transition point from the examination of the variance in Λ, shown in Fig. 4(b): in the torus region, $\alpha\leqslant\alpha_{\rm HH}$, the fluctuations in Λ are small, while for $\alpha>\alpha_{\rm HH}$, the variance is large and depends irregularly on the function of the control parameter. Unlike the case of band-merging or widening crises [23]

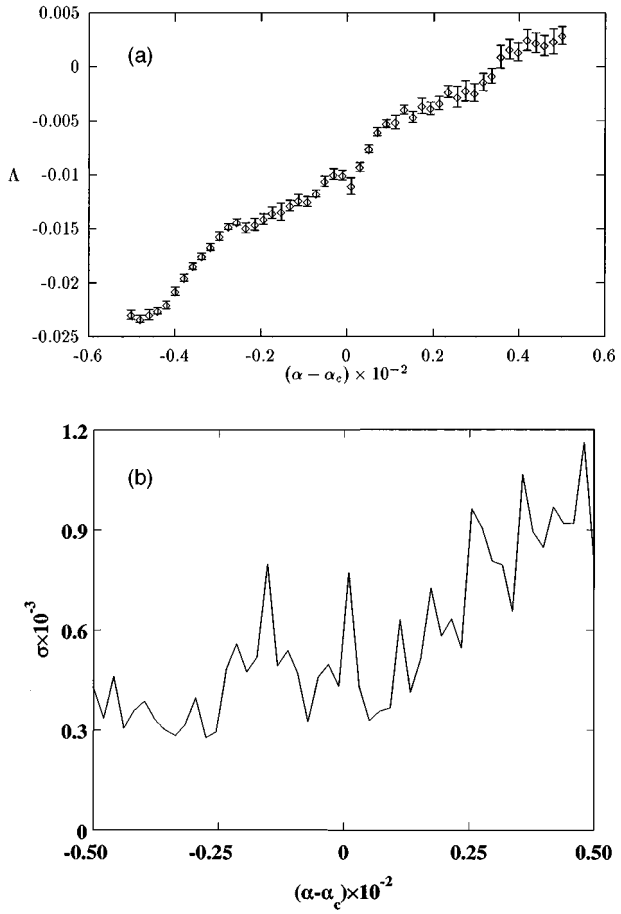

FIG. 5. The transition from a period-1 torus to one-band SNA via the fractalization route along the line $\epsilon' = 1$ and at $\alpha_F = 2.6526\ldots$. (a) Behavior of Λ through the transition, and (b) the variance.

there is no distinctive signature in the variation of the Lyapunov exponent itself (except for a certain irregularity in the SNA phase).

2. The fractalization mechanism

During fractalization, a period-k torus attractor gets wrinkled and eventually forms a k-band SNA [12]. There is no apparent interaction with unstable periodic orbits in contrast to the HH case, and there are no analogs of any crisis-like behavior. The variation of the Λ and its variance at such a transition are shown in Figs. 5(a) and 5(b), respectively, as α changes through $\alpha_F = 2.6526\ldots$ at $\epsilon' = 1$. The behavior of variance in Fig. 5(b) is similar to that of the HH case [Fig. 4(b)], except in the magnitude of the fluctuations. These figures also show that the transition from torus to SNA is smooth with no particular signature in Λ.

3. The intermittency route

Intermittent SNAs are morphologically quite distinct from those formed through other mechanisms. An example of the transition to such SNAs is shown in Fig. 6. The behavior of Λ as α is reduced through $\alpha_I = 3.405\,808\,806\ldots$ at $\epsilon' = 1$ [Fig. 6(a)] is distinctive and may be contrasted with Figs. 4(a) and 5(a). The torus which exists for $\alpha > \alpha_I$ and the intermittent SNA are depicted in Figs. 6(b) and 6(c), respectively. On the intermittent SNA, most points remain near the parent torus, with sporadic large deviations. On fractalized SNAs points on the attractor stay close to the parent fractal torus (Fig. 1 of Ref. [7]), while on HH SNAs, points are distributed within the entire region enclosed by the wrinkled bounding tori (see Fig. 1 of Ref. [5]). The other characteristic behavior can be extracted from Fig. 6(d) where we plot the variance: this changes abruptly at the transition, where a saddle-node bifurcation occurs showing the characteristic signature of the intermittency route to SNAs.

4. Finite-time Lyapunov exponents

As is well known, while Λ is negative on a SNA, for short times, the local Lyapunov exponent can be positive. One of the characteristics of the SNAs born through different mechanisms is the difference in the distribution of finite-time exponents, namely, $P(N,\lambda)$. In the limit of large N, it is clear that this distribution will collapse to a δ function, $\lim_{N\to\infty} P(N,\lambda) \to \delta(\Lambda - \lambda)$. The deviations from—and the approach to—the limit can be very different for SNAs created through different mechanisms.

Shown in Figs. 7(a)–7(c) are the distributions for $P(50,\lambda)$ across the three transitions discussed above, namely on the tori and corresponding SNAs. A common feature of all three cases is that $P(N,\lambda)$ is strongly peaked about Λ when the attractor is a torus, but on the SNA, the distribution picks up a tail which extends into the $\lambda > 0$ region. This tail directly correlates with the enhanced fluctuation in Λ on SNAs [see Fig. 4(b), 5(b), or 6(d)]. On the fractalized SNA, the distribution shifts continuously to larger Λ, but the shape remains the same for $\alpha \langle \alpha_I$ and $\alpha \rangle \alpha_I$, while on the HH or intermittent SNA, the actual shapes of the distribution on the torus and the SNA are very different.

One remarkable feature of intermittent SNAs is that the positive tail in the distribution decays very slowly: even for N as large as 10^4, it does not completely disappear [18]. In order to quantify this, we define the fraction of positive local Lyapunov exponents as

$$F_+(N) = \int_0^\infty P(N,\lambda)\, d\lambda, \tag{9}$$

and similarly, the first moment, namely, a local Kolmogorov-Sinai (KS) entropy,

$$K(N) = \int_0^\infty \lambda P(N,\lambda)\, d\lambda. \tag{10}$$

Clearly, $\lim_{N\to\infty} F_+(N) \to 0$ and $\lim_{N\to\infty} K(N) \to 0$. Empirically we have found that on the intermittent SNA, these quantities show the large N behavior

$$F_+(N) \sim N^{-\beta} \tag{11}$$

[similarly for $K(N)$] while for the fractalized or HH SNAs, the approach is exponentially fast,

$$F_+(N) \sim \exp(-\gamma N). \tag{12}$$

The exponents β and γ depend strongly on the parameters α and ϵ'. For the SNAs discussed above, we have calculated $F_+(N)$ for large N [see Fig. 7(d)] and obtain $\beta \approx 0.2$, $\gamma_{\rm HH} \approx 0.02$, and $\gamma_{\rm I} \approx 0.03$. $K(N)$ also has a similar slow fall

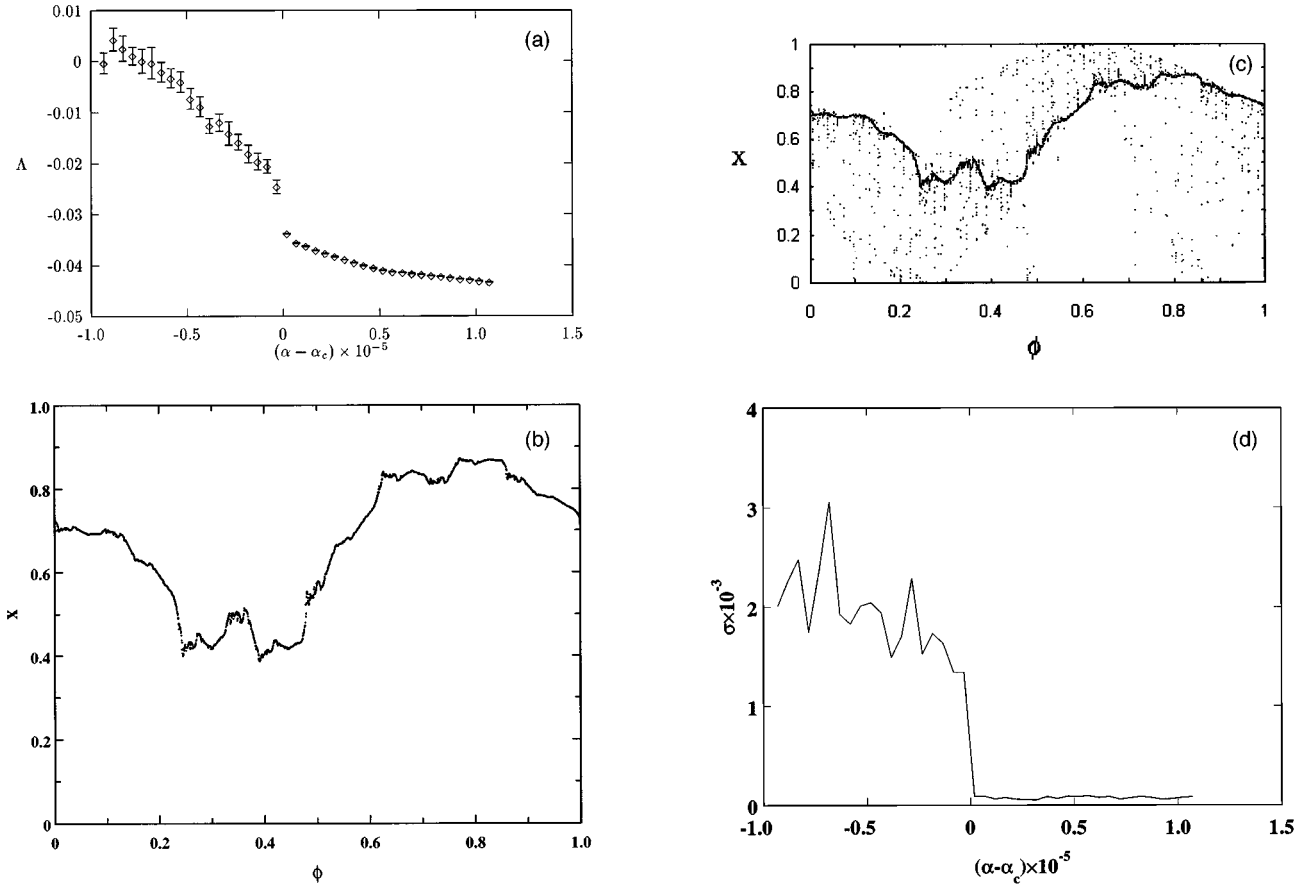

FIG. 6. The transition from a period-1 torus to one-band SNA via the intermittent transition, along the line $\epsilon'=1$ and at $\alpha_I=3.405\,808\,806\ldots$. (a) Behavior of Λ through the transition, (b) plot of the period-1 torus at $\alpha=3.405\,809$, (c) the intermittent SNA at $\alpha=3.405\,808$, (d) the variance through the transition.

off at large N for the intermittent SNA $K(N)\sim N^{-\beta'}$ with $\beta'\approx 0.55$, while for the other SNAs, the decay is slow for small N but exponential for large N.

B. Scaling at the intermittency transition

The intermittency transition from a torus to a SNA is characterized by scaling behavior for the dynamics, similar to corresponding behavior in the unforced case [24]. The ''laminar'' phase in this case is the torus, while the ''chaotic'' phase is the nonchaotic attractor. In order to obtain the distribution time in these phases, we coevolve two trajectories with identical (x_0,ϕ_0) and ϵ', with different α: since the angular coordinate remains identical, the distance between the trajectories is simply the difference in the x_n's. We calculate the time between bursts and fit to the scaling form

$$\tau\sim(\alpha_c-\alpha)^{-\theta}. \tag{13}$$

The numerical value obtained for the attractor with α near α_I and $\epsilon'=1$ is $\theta=0.52\pm 0.03$ and $\epsilon'=0.65$ is $\theta=0.5\pm 0.03$ [see Fig. 8(a)]. This suggests that the intermittency is type I.

The Lyapunov exponent itself shows the scaling form [18]

$$\Lambda-\Lambda_c\sim(\alpha_c-\alpha)^{\mu} \tag{14}$$

at fixed ϵ' which can be compared with the probability density [23,25,26] in the SNA burst phase [Fig. 8(b)]. Both these quantities have the same exponent $\mu=0.37\pm 0.03$ at $\epsilon'=1$. Although other SNAs also show intermittencylike dynamical behavior, the scaling form Eq. (14) obtains *only* for the intermittent SNAs, thus providing a means of distinguishing these from HH or fractalized SNAs.

C. Merging of SNAs

As the parameters α and ϵ are varied, the attractors of the quasiperiodically driven system undergo transformation in a manner which is analogous to the undriven chaotic system. Similar to reverse bifurcations or band merging in 1D maps, n-band SNAs transform to $n/2$-band SNAs. Through such a transition, when the dynamics remains nonchaotic and strange, Λ is a good order parameter. Sosnovtseva *et al.* [11], who discovered an example of this transition in the driven Hénon and circle maps, demonstrated the merging by examining the phase portait.

Given the fairly narrow range over which SNAs exist in any system, this transition also occurs in a restricted range. We find that the SNA bands that are formed by the HH mechanism typically do not merge at negative Lyapunov exponent, but only do so at higher driving, when they collide in the chaotic region as at a proper analog of the band-merging crisis [2]. However, the variation of Λ at such transitions

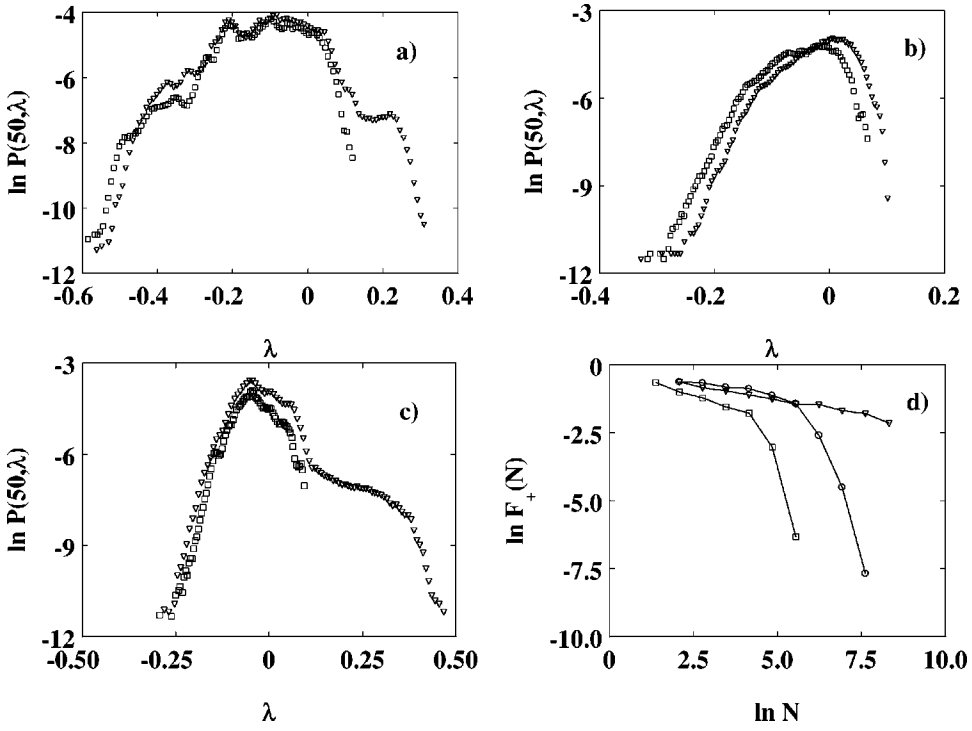

FIG. 7. Distribution of finite-time Lyapunov exponents across the three transitions. Shown are the distributions of $P(50,\lambda)$ before and after the transitions, namely, on the tori and on the SNA. (a) Along the HH route, on the torus at $\alpha=3.4874$ (□) and on the SNA at $\alpha=3.488$ (△) for $\epsilon'=0.3$. (b) Along the fractalization route, on the torus at $\alpha=2.63$ (□) and the SNA at $\alpha=2.66$ (△) for $\epsilon'=1$. (c) Along the intermittency route, on the torus at $\alpha=3.405\,81$ (□) and on the SNA at $\alpha=3.405\,805\,6$ (△) for $\epsilon'=1$. (d) Variation of $F_+(N)$ for the three different SNAs in (a), (b), and (c) showing exponential decay in the first two cases, and a power-law decay for the intermittent SNA. The respective symbols are □, ○, and ▽.

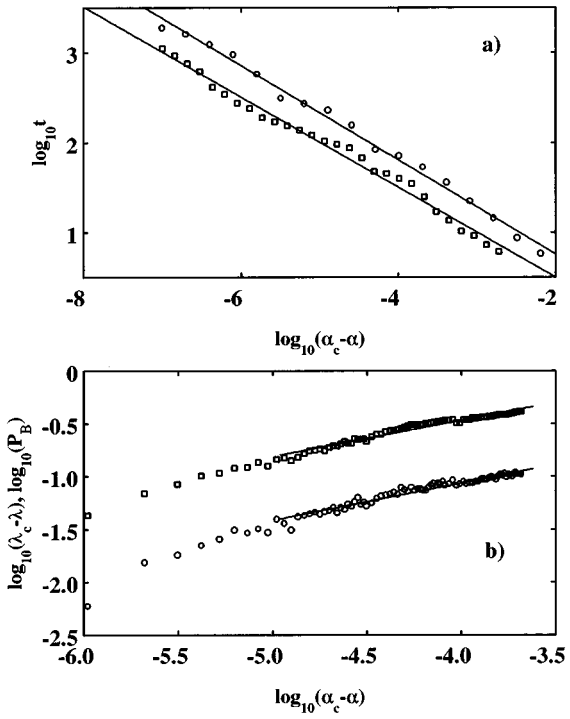

FIG. 8. Scaling behavior on the intermittent SNA. (a) Plot of the average time between bursts vs $(\alpha_c-\alpha)$ at $\epsilon'=1$ (○) and at $\epsilon'=0.65$ (□). (b) The probability density (p_B) in the burst phase (○) and Λ (□) vs $(\alpha_c-\alpha)$ at $\epsilon'=1$. The measured exponents are $\mu\approx 0.37$.

does not follow a uniform pattern as in the unforced case [23,24].

Those SNAs which are formed via fractalization may merge at negative Λ. Figure 9(a) shows the variation of Λ for such an example of a two-band SNA merging to a one-band SNA. The Lyapunov exponent *decreases* with increasing nonlinearity. The distribution for short time Lyapunov exponents before and after the SNA band-merging crisis confirms that the distribution shifts to lower λ; see Fig. 9(b). Both these figures indicate that the chaoticity of the system [measured either through local (λ_N) or global (Λ) indicators] becomes significantly lower after merging crisis. This band merging is different from the unforced case [17,24] where Λ generally increases as number of bands decreases with increasing nonlinearity.

D. The effect of noise

An important consideration in the study of SNAs is their robustness. Given the somewhat unusual properties of such attractors and the fact that they exist over small regions in parameter space, it is natural to examine the effect of fluctuations. This is of particular relevance with respect to the experimental observation of SNAs [14,16]. The effect of noise in the logistic map has been extensively studied [24], and it is known that noise generally lowers the threshold for chaos—systems with additive noise have a larger Lyapunov exponent for smaller nonlinearity. Furthermore, transitions and bifurcations get ''blurred'' in the presence of fluctuations.

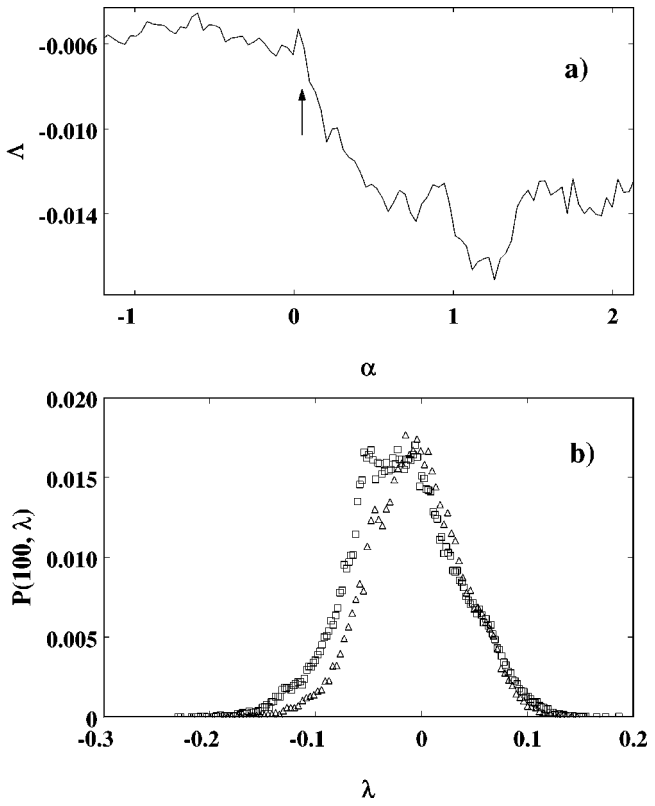

FIG. 9. (a) Variation of Λ at band-merging bifurcation in SNA for two-band SNAs to a one-band SNA along $\epsilon=0.05$. (b) Distribution of local Lyapunov exponents, $P(100,\lambda)$, across the merging transition in (a) which takes place at $\alpha_c \approx 3.387\,439$.

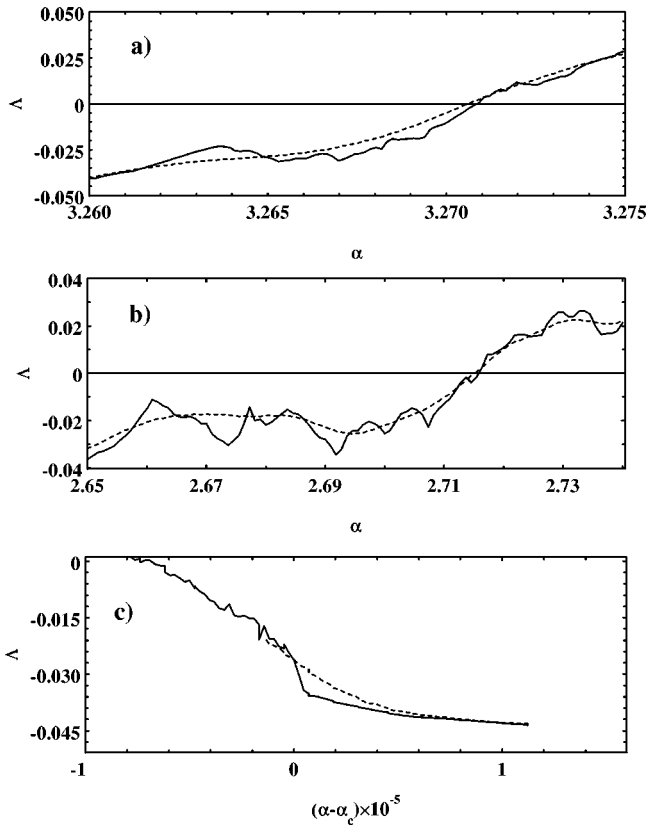

FIG. 10. The shift in Λ with additive noise near the threshold for the transition from SNA to chaos for the cases of (a) HH, (b) fractalization, for $\rho=0$ (solid line), 10^{-3} (dashed line) and (c) intermittent SNAs, $\rho=0$ (solid line), $\rho=10^{-5}$ (dashed). All quantities are estimated from a set of 50 samples of 10^5 time steps.

To examine some of these effects, we have studied this system through the introduction of additive noise in the dynamics, for example as

$$x_{n+1}=\alpha[1+\epsilon\,\cos(2\pi\phi_n)]x_n(1-x_n)+\rho\xi_n\,, \qquad (15)$$

where ρ is the noise amplitude and the random variable $\{\xi\}$ is δ correlated in time. As may have been anticipated, the addition of noise ''smears out'' tori, and the threshold values for bifurcations typically shift to lower α at fixed ϵ.

The actual transitions—now from noisy tori to noisy SNAs—survive, and examples of this are shown in Fig. 10 for fractalized, HH, and intermittent SNAs, where Λ is shown as a function of α with and without noise. Since as a function of decreasing α the intermittent SNA is born out of a torus, the effect of noise is to increase the parameter value at which this SNA is created (relative to the $\rho=0$ case) while the opposite effect, namely, a reduction of parameter value for the transition to HH and fractalized SNAs, is seen. These behaviors are typical: we have verified that SNAs in related systems such as the quasiperiodically forced ring and Hénon maps behave similarly.

Upon addition of noise, the global structures of the different types of SNAs remain similar—the qualitative behavior such as scaling, band merging, etc. are retained—although the numerical values of constants and exponents change. The degree of robustness varies with nonlinearity, though: for instance, at $\epsilon'=1$, the intermittent transition survives for additive noise of amplitude up to $\rho=10^{-6}$, while at lower ϵ' the transition is robust to even larger $\rho \approx 10^{-4}$. The region of scaling in the presence of noise is small, and the intermittency exponent varies; we have found that the numerical value of θ [see Eq. (13)] is 0.56 ± 0.04 at $\epsilon'=1$.

IV. SUMMARY

In this paper we have described the phenomenology of strange nonchaotic dynamics in a prototypical example, namely, the quasiperiodically driven logistic map. There are three different mechanisms through which SNAs can be created in this system; these routes to SNAs have their analogs in the different scenarios for the onset of chaos in dissipative dynamical systems [17].

We obtain a ''phase diagram'' for the system, delineating the different asymptotic behaviors that are possible as a function of the parameters, namely, n-frequency torus attractors, strange chaotic attractors, and SNAs. There are two major chaotic regions with different characteristics, separated from each other by a region of quasiperiodic and strange nonchaotic behavior. As a function of parameters, therefore, the system can show several transitions in the dynamics and several of these have been studied.

To distinguish among the different mechanisms through which SNAs are born, we examine not only the manner in which Λ changes as a function of parameters, but also the variance σ. These indices together give a clear indication of the transition from quasiperiodic to strange nonchaotic dynamics. We also examine the distribution of local Lyapunov

exponents, $P(N,\lambda)$ and find that on different SNAs, the fraction of positive exponents $F_+(N)$ or its moment, the local KS entropy, decay in different manners depending on the type of SNA that is formed.

In addition to three routes that have been decribed previously [5,6,8], we identify a new mechanism for the creation of SNAs. These *intermittent* SNAs [18] are atypical in that they are created at the quasiperiodic analog of a saddle-node bifurcation [17], and the signature of the transition is a discontinuous change both in Λ as well as in σ. The chaotic component on the intermittent SNA is long lived, giving rise to long chaotic transients: this shows up as a slowly decaying positive tail in $P(N,\lambda)$, and a resulting power-law decay for $F_+(N)$ or $K(N)$. (On other SNAs, in contrast, these quantities decay exponentially.) We further characterize intermittent SNAs by establishing the scaling behavior for residence times in the different phases and find that the qualitative picture is in accord with type-I intermittency [17]. This behavior persists in the presence of additive random noise.

We have described the intermittent SNA in detail and shown that both in its creation as well as in its morphology it is distinct from other SNAs, and bears some relation, in terms of the phase diagram, to a reentrant phase. (In the higher dimensional system of the forced circle map [11] for which the phase diagram has been obtained, the intermittent SNA occurs in an analogus region). In the vicinity of such attractors, a number of dynamical quantities show scaling behavior.

There are other bifurcation phenomena in such systems, and we have examined the case of SNA band merging, namely, the coalescence of different branches of a multiband attractor. At this transition, in contrast to analogous behavior in the logistic map [23], Λ, which remains negative throughout, decreases. A clear understanding of why this is so is not available at present.

In summary, our primary emphasis has been on the use of a number of Lyapunov measures—the largest nontrivial Lyapunov exponent, its fluctuations, the distribution of finite-time Lyapunov exponents, and partial moments of this distribution—to characterize the different types of transitions to strange nonchaotic attractors that arise in the forced logistic map.

For hyperbolic systems, the theory for the Lyapunov exponent and for Lyapunov measures is well developed [27]. For SNAs, the situation is in a less satisfactory state, and our work represents initial efforts towards understanding the phenomenology of quasiperiodically driven systems. For a number of bifurcations in such systems in general, it is clear that the largest Lyapunov exponent is a good order parameter. It is likely that the considerable formalism for such transitions that has been developed for chaotic strange attractors [17,27] can be applied in large part to the strange nonchaotic regime, but the extent to which the theory carries over is an aspect that remains to be explored in future work.

ACKNOWLEDGMENT

This research was supported by Grant No. SPS/MO-5/92 from the Department of Science and Technology, India.

[1] C. Grebogi, E. Ott, S. Pelikan, and J. A. Yorke, Physica D **13**, 261 (1984).
[2] C. Grebogi, E. Ott, F. J. Romeiras, and J. A. Yorke, Phys. Rev. A **36**, 5365 (1987).
[3] F. J. Romeiras, A. Bondeson, E. Ott, T. M. Antonsen, and C. Grebogi, Physica D **26**, 277 (1987).
[4] S. P. Kuznetsov, A. S. Pikovsky, and U. Feudel, Phys. Rev. E **51**, R1629 (1995).
[5] J. F. Heagy and S. M. Hammel, Physica D **70**, 140 (1994).
[6] K. Kaneko, Prog. Theor. Phys. **71**, 1112 (1984).
[7] T. Nishikawa and K. Kaneko, Phys. Rev. E **54**, 6114 (1996).
[8] T. Yalçinkaya and Y. C. Lai, Phys. Rev. Lett. **77**, 5039 (1996).
[9] E. Ott and J. C. Sommerer, Phys. Lett. A **188**, 39 (1994); P. Ashwin, J. Buescu, and I. Stewart, *ibid.* **193**, 126 (1994); Y. C. Lai and C. Grebogi, Phys. Rev. E **52**, R3313 (1995).
[10] A. Pikovsky and U. Feudel, Chaos **5**, 253 (1995); U. Feudel, J. Kurths, and A. Pikovsky, Physica D **88**, 176 (1995).
[11] O. Sosnovtseva, U. Feudel, J. Kurths, and A. Pikovsky, Phys. Lett. A **218**, 255 (1996).
[12] Y. C. Lai, Phys. Rev. E **53**, 57 (1996); Y. C. Lai, U. Feudel, and C. Grebogi, *ibid.* **54**, 6070 (1996).
[13] Y. Pomeau and P. Manneville, Commun. Math. Phys. **74**, 189 (1980).
[14] W. L. Ditto, M. L. Spano, H. T. Savage, S. N. Rauseo, J. Heagy, and E. Ott, Phys. Rev. Lett. **65**, 533 (1990).
[15] T. Zhou, F. Moss, and A. Bulsara, Phys. Rev. A **45**, 5394 (1992).
[16] W. X. Ding, H. Deutsch, A. Dinklage, and C. Wilke, Phys. Rev. E **55**, 3769 (1997).
[17] E. Ott, *Chaos in Dynamical Systems* (Cambridge University Press, Cambridge, England, 1994).
[18] A. Prasad, V. Mehra, and R. Ramaswamy, Phys. Rev. Lett. **79**, 4127 (1997).
[19] This route is quite general and occurs in higher-dimensional systems as well. In the quasiperiodically forced ring map [11] (see Fig. 3 there for a phase diagram) intermittent SNAs occur (for example, at $k=3$ and $A=0.185\,146\,9$), and are apparently created by a similar saddle-node bifurcation.
[20] M. Ding, C. Grebogi, and E. Ott, Phys. Lett. A **137**, 167 (1989).
[21] T. Kapitaniak and M. S. El Naschie, Phys. Lett. A **154**, 249 (1991).
[22] K. Kaneko, Prog. Theor. Phys. **72**, 202 (1984).
[23] V. Mehra and R. Ramaswamy, Phys. Rev. E **53**, 3420 (1996).
[24] J. Crutchfield, D. Farmer, and B. Huberman, Phys. Rep. **92**, 45 (1982).
[25] R. Pompe and R. W. Leven, Phys. Scr. **38**, 651 (1988).
[26] C. Grebogi, E. Ott, and J. Yorke, Physica D **7**, 181 (1983).
[27] P. Grassberger, R. Badii, and A. Politi, J. Stat. Phys. **51**, 135 (1988).